DMD Fast Forward. Published on December 9, 2021 as DOI: 10.1124/dmd.121.000597
This article has not been copyedited and formatted. The final version may differ from this version.

**Title:** Factors Influencing Luciferase-Based Bioluminescent Imaging in Preclinical Models of Brain Tumor

**Authors:** Minjee Kim[1], Shiv K. Gupta[2], Wenjuan Zhang[1], Surabhi Talele[1], Afroz S. Mohammad[1], Janice Laramy[1], Ann C. Mladek[2], Shuangling Zhang[1], Jann N. Sarkaria[2], and William F. Elmquist[1]

Affiliations

[1]Brain Barriers Research Center, Department of Pharmaceutics, College of Pharmacy, University of Minnesota, Minneapolis, Minnesota, USA (MK, WZ, ST, ASM, JKL, SZ, WFE)

[2]Department of Radiation Oncology, Mayo Clinic, Rochester, Minnesota, USA (SG, ACM, JNS)

DMD Fast Forward. Published on December 9, 2021 as DOI: 10.1124/dmd.121.000597
This article has not been copyedited and formatted. The final version may differ from this version.

**Running title**

CNS distribution of luciferase substrates

**Corresponding author**

William F. Elmquist

Professor

Department of Pharmaceutics

University of Minnesota

308 Harvard ST SE

Minneapolis MN 55455

Phone: 612-625-0097; fax: 612-626-2125

e-mail: elmqu011@umn.edu

DMD Fast Forward. Published on December 9, 2021 as DOI: 10.1124/dmd.121.000597
This article has not been copyedited and formatted. The final version may differ from this version.

Number of text pages: 40

Number of tables: 3

Number of figures: 6

Number of references: 37

Number of words in abstract: 193

Number of words in introduction: (excluding in-text citations) 917

Number of words in discussion: (excluding in-text citations) 2290

Abbreviations

AUC, area under the curve

BAT, brain around tumor

BBB, blood-brain barrier

Bcrp, breast cancer resistance protein

BKO, Bcrp knockout (*Bcrp1*$^{-/-}$)

BLI, bioluminescent imaging

CL, clearance

CL/F, apparent clearance

DA, distribution advantage

fLuc, firefly luciferase

DMD Fast Forward. Published on December 9, 2021 as DOI: 10.1124/dmd.121.000597
This article has not been copyedited and formatted. The final version may differ from this version.

FVB, Friend leukemia virus strain B

GBM, glioblastoma

IC, intracranial

$IC_{50}$, the half maximal inhibitory concentration

Kp, tissue-to-plasma ratio

Kpuu, unbound (free) tissue-to-plasma ratio

LC-MS/MS, liquid chromatography–tandem mass spectrometry

MDCKII, Madin-Darby Canine Kidney II

MRPs, multidrug resistance-associated proteins

NB, normal brain

NCA, noncompartmental analysis

Papp, apparent permeability coefficient

PDX, patient-derived xenograft

RED, rapid equilibrium dialysis

WT, wild-type

DMD Fast Forward. Published on December 9, 2021 as DOI: 10.1124/dmd.121.000597
This article has not been copyedited and formatted. The final version may differ from this version.

**Abstract**

Bioluminescent imaging (BLI) is a powerful tool in biomedical research to measure gene expression and tumor growth. The current study examined factors that influence the BLI signal, specifically focusing on the tissue distribution of two luciferase substrates, D-luciferin and CycLuc1. D-luciferin, a natural substrate of firefly luciferase, has been reported to have limited brain distribution, possibly due to the efflux transporter, breast cancer resistance protein (Bcrp), at the blood-brain barrier. CycLuc1, a synthetic analog of D-luciferin, has a greater BLI signal at lower doses than D-luciferin, especially in the brain. Our results indicate that limited brain distribution of D-luciferin and CycLuc1 is predominantly dictated by their low intrinsic permeability across the cell membrane, where the efflux transporter, Bcrp, plays relatively minor role. Both genetic ablation and pharmacological inhibition of Bcrp decreased the systemic clearance of both luciferase substrates, significantly increasing exposure in the blood and, hence, in organs and tissues. These data also indicate that the biodistribution of luciferase substrates can be differentially influenced in luciferase-bearing tissues, leading to a “tissue-dependent” BLI signal. The results of this study point to the need to consider multiple mechanisms that influence the distribution of luciferase substrates.

DMD Fast Forward. Published on December 9, 2021 as DOI: 10.1124/dmd.121.000597
This article has not been copyedited and formatted. The final version may differ from this version.

## Significance Statement

Bioluminescence is used to monitor many biological processes, including tumor growth. This study examined the pharmacokinetics, brain distribution, and the role of active efflux transporters on the luciferase substrates, D-luciferin and CycLuc1. CycLuc1 has a more sustained systemic circulation time (longer half-life), that can provide an advantage for the superior imaging outcome of CycLuc1 over D-luciferin. The disparity in imaging intensities between brain and peripheral sites is due to low intrinsic permeability of these luciferase substrates across the blood-brain barrier.

DMD Fast Forward. Published on December 9, 2021 as DOI: 10.1124/dmd.121.000597
This article has not been copyedited and formatted. The final version may differ from this version.

## Introduction

Bioluminescent imaging (BLI) is commonly used to visualize gene expression in biomedical research and to measure tumor burden in preclinical cancer research (Thorne et al., 2010). The most common reporter used is firefly luciferase (fLuc) combined with D-luciferin. D-luciferin is oxidized by fLuc in the presence of adenosine triphosphate (ATP) and magnesium cofactors (Kaskova et al., 2016). This enzymatic reaction happens in multiple steps. First, D-luciferin is transformed to luciferyl adenylate, and this central intermediate is then converted through a series of intermediates to ultimately form oxyluciferin that releases a photon (bioluminescence). Beyond the fLuc/D-luciferin pair, there are numerous native or sequence-optimized bioluminescent enzymes that can be coupled with natural or synthetic substrates to provide a spectrum of light emission characteristics that are optimized for various uses.

There are several factors that affect the light signal measurements (Figure 1) when whole animal BLI is performed. (1) Pharmacokinetics and biodistribution of luciferase substrates are crucial in the eventual production of the light signal in the target area of imaging in animals. Luciferase substrates, often administered to the animal by intraperitoneal injection, need to be adequately delivered to the tissue where the luciferase enzyme is expressed. (2) Once adequately distributed to the target tissue, luciferase substrates need to diffuse into the cell which is dictated by membrane permeability where the luciferase enzyme is expressed. (3) The physicochemical

DMD Fast Forward. Published on December 9, 2021 as DOI: 10.1124/dmd.121.000597
This article has not been copyedited and formatted. The final version may differ from this version.

parameters, such as enzyme affinity for the substrate, Km, and activity of the enzyme at the target area of imaging, critically affects the rate of reaction (light signal intensity) according to Michaelis-Menten kinetics. (4) Tissue penetration of emitted light is especially important for *in vivo* imaging. The light wavelength can dramatically affect attenuation of light intensity between the location of photon production in biological tissues and the photon detection device; longer or red-shifted wavelengths are known to penetrate typical tissue better in part due to less attenuation anticipated (Dawson et al., 1980; Weissleder and Ntziachristos, 2003; Jathoul et al., 2014). (5) The sensitivity of a detector or camera can also influence the signal intensities measured.

D-luciferin has been used extensively as a tool substrate in neuroscience research for non-invasive imaging despite limitations of its distribution across the blood-brain barrier (BBB) (Berger et al., 2008). The limited distribution of D-luciferin into the brain is considered due to activity of the breast cancer resistance protein (Bcrp) efflux transporter in the luminal membrane of brain capillary endothelial cells (Zhang et al., 2007; Bakhsheshian et al., 2013). Bcrp is one of several efflux transporters that translocate xenobiotics from the intracellular compartment of endothelial cells back into the capillary lumen, and previous mouse studies have demonstrated enhanced BLI signal from the brain when mice were co-dosed with a pharmacologic Bcrp inhibitor (Bakhsheshian et al., 2013). Recently, a synthetic analogue of D-luciferin, CycLuc1, was reported as an alternative substrate of fLuc that results in superior imaging results for the

DMD Fast Forward. Published on December 9, 2021 as DOI: 10.1124/dmd.121.000597
This article has not been copyedited and formatted. The final version may differ from this version.

purpose of brain imaging in neuroscience research (Evans et al., 2014). The structure and physicochemical properties are similar between CycLuc1 and D-luciferin, where the main difference is the higher lipophilicity of CycLuc1 (XLogP 2.6) compared to D-luciferin (XLogP 0.9) (Table S1). More intense light output was observed for CycLuc1 than D-luciferin at the same molar concentration (Reddy et al., 2010). The increased relative quantum yield of CycLuc1, as the authors hypothesized, might be due to the increased rigidity and restricted bond rotation of the CycLuc1 structure (Table S1). Another distinctive and important characteristic of CycLuc1 is the much lower Km with firefly luciferase (Km for D-luciferin and CycLuc1, 6.76 μM and 0.1 μM, respectively) (Harwood et al., 2011). Consistent with these metrics, CycLuc1 provided a much brighter signal at a significantly lower dose than D-luciferin in a mouse imaging model in which an fLuc-expressing virus was injected into a deep brain structure. Considering the known limitations of D-luciferin distribution into brain and enhanced lipophilicity of CycLuc1, these results were interpreted as an evidence of superior distribution of CycLuc1 across the blood-brain barrier (BBB) (Reddy et al., 2010). The focus of the present study is to critically evaluate this hypothesis or otherwise explain the superior neuro-imaging characteristics of CycLuc1.

The distributional and pharmacokinetic properties of these luciferase substrates were compared by directly measuring the concentrations of both D-luciferin and CycLuc1 by liquid chromatography–tandem mass spectrometry (LC-MS/MS) in various tissues,

DMD Fast Forward. Published on December 9, 2021 as DOI: 10.1124/dmd.121.000597
This article has not been copyedited and formatted. The final version may differ from this version.

including brain and plasma. This is a novel approach, since concentrations of luciferase substrates have been predicted in many previous publications solely based on their BLI light signal intensities. However, the signal intensity of light can be influenced by various factors (Figure 1) in addition to the concentration of substrates at the site of action, as previously described. Therefore, the direct determination of substrate concentrations by using LC-MS/MS provides a more robust measure of the biodistribution and pharmacokinetics of luciferase substrates, which then critically informs their use in biomedical research.

In the current study, several specific questions were examined to understand the distribution of luciferase substrates and the possible reasons for the enhanced light signal from CycLuc1. First, the intensity of BLI signal with D-luciferin and CycLuc1 was compared in heterotopic and orthotopic xenografts of a patient-derived glioblastoma (GBM) model. Second, the permeability of substrates across a cell monolayer and efflux liabilities of both compounds with respect to Bcrp-mediated transport were examined by using *in vitro* experiments in Bcrp-transfected cells. Third, the role of Bcrp on the brain distribution of D-luciferin and CycLuc1 was studied *in vivo* using Bcrp knockout mice. Fourth, the influence of efflux transporter inhibitors was examined to investigate the role of transporters on D-luciferin and CycLuc1 biodistribution. The answers to these specific questions, as discussed in the current study, provide a better understanding and

DMD Fast Forward. Published on December 9, 2021 as DOI: 10.1124/dmd.121.000597
This article has not been copyedited and formatted. The final version may differ from this version.

interpretation of the use of BLI markers, and give more general guidance when choosing a substrate for luciferase-based reporter systems for *in vivo* imaging.

## Materials and Methods

### Chemicals and reagents

(S)-2-(6-Hydroxy-2-benzothiazolyl)-2-thiazoline-4-carboxylic acid, 4,5-Dihydro-2-(6-hydroxy-2-benzothiazolyl)-4-thiazolecarboxylic acid (D-luciferin) was purchased from Thermo Fisher Scientific (Waltham, MA). (4R)-2-(6,7-dihydro-5H-pyrrolo[3,2-f][1,3]benzothiazol-2-yl)-4,5-dihydro-1,3-thiazole-4-carboxylic acid (CycLuc1) was purchased from Millipore (Burlington, MA). 17-(Cyclopropylmethyl)-6,7-dehydro-4,5α-epoxy-3,14-dihydroxy-6,7-2',3'-indolomorphinan hydrochloride (Naltrindole) was purchased from Tocris Bioscience (Ellisville, MO). All other chemicals and reagents used were high-performance liquid chromatography grade from Thermo Fisher Scientific (Waltham, MA). The rapid equilibrium dialysis (RED) base plate and membrane inserts (8 kDa molecular weight cut-off cellulose membrane) were purchased from Thermo Fisher Scientific (Waltham, MA).

### Lentiviral vector and cell transduction

A modified lentivirus vector, pGIPZ-Luc2-td-tomato, was developed by replacing turbo green fluorescent protein tag of pGIPZ with a fusion of firefly luciferase (Luc2) and

DMD Fast Forward. Published on December 9, 2021 as DOI: 10.1124/dmd.121.000597
This article has not been copyedited and formatted. The final version may differ from this version.

tandem tomato (td-tomato) red fluorescent protein excised from pcDNA3.1(+)/Luc2-td-tomato and lentiviral packaging and transduction of primary GBM6 cells was performed as previously described (Laramy et al., 2017).

### *In vivo* tumor xenograft mouse model

All animal studies were approved by the Institutional Animal Care and Use Committee. For subcutaneous xenograft model, GBM6-Luc2-td-tomato cells were suspended in Matrigel/PBS and injected in the flank of athymic nude mice with 2 x $10^6$ cells. For orthotopic models, cells (3x$10^5$) were directly injected in to the right basal ganglia of anesthetized athymic nude mice (athymic Ncr-nu/nu, National Cancer Institute, Frederick, MD) using a small animal stereotactic frame (ASI Instruments, Houston, TX) as previously described (Kim et al., 2018).

### *In vivo* BLI

6-week-old female athymic nude mice with established tumor xenografts were anesthetized by isoflurane inhalation and maintained under anesthesia by continuous inhalation of isoflurane until imaging was complete. BLI signal from the tumor was measured weekly with either D-luciferin (Gold Biotechnology) or CycLuc1, ten minutes after a single intraperitoneal injection of these substrates, animal were imaged by IVIS Spectrum. The conditions for BLI acquisition were as follows: open emission filter,

DMD Fast Forward. Published on December 9, 2021 as DOI: 10.1124/dmd.121.000597
This article has not been copyedited and formatted. The final version may differ from this version.

exposure time 60 seconds, binning medium for 8, field of view 12.9 cm, and f/stop as 1. Images were analyzed for total flux with Living Image 4.3 software (PerkinElmer).

### *In vitro* trans-well permeability assay

*In vitro* bi-directional flux assay was performed with Madin-Darby Canine Kidney II (MDCKII) cells that overexpress Bcrp or a vector control. Both cell lines were kindly provided by Dr. Alfred Schinkel. Cells were cultured in Dulbecco's modified Eagle's medium (DMEM) supplemented with 10% (v/v) fetal bovine serum and antibiotics (penicillin, 100 U/ml; streptomycin, 100 mg/ml; amphotericin B, 250 ng/ml). Cells were seeded on the permeable polyester membrane transwell inserts (12 mm diameter with 0.4 μm pore size) in 12-well plate (Corning™, Corning, NY) with a density of 1 x $10^5$ cells/well, and cultured for 7 days. The average values of transepithelial electrical resistance (TEER) on day 7 were about 280 Ω/$cm^2$. On the day of experiment, cells were washed with serum free cell assay buffer twice and pre-incubated with or without inhibitor, ko-143, for 30 minutes. Buffer with specified concentrations of either D-luciferin or CycLuc1 was added to the donor compartments. For apical to basolateral transport, 0.4 ml of substrate containing buffers were added to the apical (top) compartment, and for basolateral to apical transport, 1.2 ml of drug containing buffers were added to the basolateral (bottom) compartment. The blank buffer without D-Luciferin or CycLuc1 was added to the receiver compartments. Immediately after the start of incubation, 10 μL of buffer was collected from the donor compartments. Plates were incubated in orbital

DMD Fast Forward. Published on December 9, 2021 as DOI: 10.1124/dmd.121.000597
This article has not been copyedited and formatted. The final version may differ from this version.

shaker at 37°C, and 50 µL of buffer samples were collected from the receiver compartments at 60, 90, and 120 minutes after incubation, and blank buffer without D-Luciferin or CycLuc1 was added to the receiver compartments at each time point. After 120 minutes, the integrity of the cell monolayer was confirmed with lucifer yellow. All samples were store at -80°C until the LC-MS/MS analysis.

Apparent permeabilities of D-luciferin and CycLuc1 were determined by the following equation;

$$\text{Apparent permeability (Papp)} = \frac{dQ/dt}{C0 \times A} \qquad \text{(Equation 1)}$$

where *dQ/dt* is the change of mass transported across the cell monolayer over time, *C0* is the concentration of analyte (D-luciferin or CycLuc1) in the donor compartment at time zero, and *A* is the surface area of the monolayer cell.

Efflux ratios of D-luciferin and CycLuc1 were calculated by the following equation;

$$\text{Efflux ratio (ER)} = \frac{\text{Papp from basolateral to apical compartment}}{\text{Papp from apical to basolateral compartment}} \qquad \text{(Equation 2)}$$

**Free fraction in mouse plasma and brain homogenate**

The free fractions of D-luciferin and CycLuc1 in mouse plasma and mouse brain homogenate were examined by using RED device. The brain homogenate was prepared by mechanical homogenization after adding 2 volumes (w/v) of phosphate buffer saline (PBS; pH 7.4). Mouse plasma or brain homogenate mixed with 5 µM of D-luciferin or CycLuc1 was loaded into the sample chamber separated by a cellulose membrane insert

DMD Fast Forward. Published on December 9, 2021 as DOI: 10.1124/dmd.121.000597
This article has not been copyedited and formatted. The final version may differ from this version.

(8000 Da cut off), and blank PBS buffer was loaded into the receiver chamber (*N*=5). The apparatus was sealed and incubated at 37°C for 4 hours in an orbital shaker with a 300 rpm agitation. Samples were collected at the end of incubation from each chamber and stored at -80°C until LC-MS/MS analysis. Undiluted free fraction in the brain was extrapolated with the previously reported equation listed below (Kalvass and Maurer, 2002) using the dilution factor (D) of 3:

$$\text{Free fraction (fu)} = \frac{1/D}{\left(\left(\frac{1}{fu,diluted}\right)-1\right)+1/D} \qquad \text{(Equation 3)}$$

The unbound (free) concentration of D-luciferin or CycLuc1 partitioning into the brain was determined by the equation below:

$$\text{Free brain partition coefficient (Kp,uu)} = \frac{\text{free brain concentration}}{\text{free plasma concentration}} = K_{p,brain} \times \frac{fu_{,brain}}{fu_{,plasma}}$$

(Equation 4)

where $Kp_{,brain}$ is the brain-to-plasma ratio based on area under the total concentration time profile.

### *In vivo* Pharmacokinetic Studies

#### Animals

Friend leukemia virus strain B (FVB) wild-type (WT) and Bcrp knockout (*Bcrp1*$^{-/-}$, BKO) mice were used for *in vivo* studies (Taconic Farms, Germantown, NY). Mice used for the experiments were in 8 to 16 weeks old with approximate weight of 15 to 35 g at

DMD Fast Forward. Published on December 9, 2021 as DOI: 10.1124/dmd.121.000597
This article has not been copyedited and formatted. The final version may differ from this version.

the time of experiment and balanced for sex. The animals used for pharmacokinetic and inhibitor studies were maintained and housed in the American Association for the Accreditation of Laboratory Animal Care (AAALAC International) accredited Research Animal Resources (RAR) facility located at the Academic Health Center, University of Minnesota, following an approved breeding protocol. All experimental protocols were approved by the University of Minnesota Institutional Animal Care and Use Committee (IACUC) and conducted in accordance with the Guide for the Care and Use of Laboratory Animals established by the U.S. National Institutes of Health (Bethesda, MD).

**Full time course pharmacokinetic studies**

Since D-luciferin and CycLuc1 are light sensitive, all study procedures and sample collections were performed in a dark room with minimal exposure to the dim light. A single dose of either D-luciferin or CycLuc1 was administered by either intraperitoneal injection or tail vein injection to WT and BKO FVB mice. The dosing solutions for both compounds were prepared in sterile water with 1% DMSO. Following euthanasia in a carbon dioxide chamber, blood and brain samples were collected at the pre-determined time points ranging from 5 minutes to 180 minutes after intravenous injection or from 2 minutes to 60 minutes after single intraperitoneal injection (N=3-5 at each time point). Mouse whole blood was collected by cardiac puncture using heparinized syringes and immediately transferred to heparinized tubes. The plasma was separated by

DMD Fast Forward. Published on December 9, 2021 as DOI: 10.1124/dmd.121.000597
This article has not been copyedited and formatted. The final version may differ from this version.

centrifugation at 6500 rpm at 4°C for 20 minutes. Plasma and brain were stored at -80°C until LC-MS/MS analysis.

**Transporter inhibitor studies**

Transporter inhibitors, Ko-143 or probenecid, were dosed by intravenous bolus injection either 10 minutes (Ko-143) or 30 minutes (probenecid) prior to the administration of D-luciferin or CycLuc1. Doses used for the inhibitor studies were as follows; 16 mg/kg of Ko-143, 150 mg/kg of probenecid, 50 mg/kg of D-luciferin, and 10 mg/kg for CycLuc1. Blood and brain samples were collected at 10 minutes and 60 minutes post-dose using the same euthanasia and sample collection procedures as described above.

**Pharmacokinetic data analysis**

Concentration-time profiles of D-luciferin and CycLuc1 were analyzed by using Phoenix WinNonlin version 6.4 (Certara USA Inc., Princeton, NJ), and pharmacokinetic parameters and metrics were calculated by non-compartmental analysis (NCA). The terminal elimination rate constants were determined by using the last three to four points in the concentration-time profiles. The brain-to-plasma partition coefficients ($Kp_{,brain}$) were calculated as below:

$$\text{Brain partition coefficient } (Kp_{,brain}) = \frac{AUC_{brain}}{AUC_{plasma}} \qquad \text{(Equation 5)},$$

DMD Fast Forward. Published on December 9, 2021 as DOI: 10.1124/dmd.121.000597
This article has not been copyedited and formatted. The final version may differ from this version.

where $AUC_{brain}$ is an area under the curve from time zero to infinity of brain concentration-time profile ([$AUC_{(0\rightarrow\infty),\ brain}$]) and $AUC_{plasma}$ is an area under the curve plasma concentration-time profile ([$AUC_{(0\rightarrow\infty),\ plasma}$]). The distribution advantages (DA) of brain in BKO mice were determined by the ratio of brain partition coefficients in knockout mice to that in WT mice. The bioavailability of D-luciferin and CycLuc1 following an intraperitoneal injection was calculated as below:

$$\text{Intraperitoneal bioavailability } (F) = \left\{ \frac{\left[AUC_{(0\rightarrow\infty),\ plasma}\right]_{IP}}{\left[AUC_{(0\rightarrow\infty),\ plasma}\right]_{IV}} \right\} \qquad \text{(Equation 6)}$$

where the $\left[AUC_{(0\rightarrow\infty),\ plasma}\right]_{IP}$ is the area under the curve from time zero to infinity of plasma concentration-time profile following a single intraperitoneal dose and $\left[AUC_{(0\rightarrow\infty),\ plasma}\right]_{IV}$ is the area under the curve from time zero to infinity of plasma concentration-time profile following a single intravenous dose.

**Analytical LC-MS/MS bioanalysis**

Total concentrations of both D-luciferin and CycLuc1 in samples were determined by using high performance liquid chromatography (Agilent model 1200 separation system; Agilent Technologies, Santa Clara, CA) coupled with TSQ Quantum triple quadrupole mass spectrometer (Thermo Finnigan, San Jose, CA). For liquid chromatographic separation, gradient elution was implemented using Phenomenex Synergi Polar-RP column (75 X 2 mm, 4 μm). The initial composition of the mobile phase was comprised of 75% distilled water with 0.1% formic acid (A) and 25% acetonitrile with 0.1% formic acid

DMD Fast Forward. Published on December 9, 2021 as DOI: 10.1124/dmd.121.000597
This article has not been copyedited and formatted. The final version may differ from this version.

(B) with a 0.2 ml/min flow rate. The total run time was 11 minutes, and retention times for D-luciferin, CycLuc1, and naltrindole (internal standards) were 1.5, 1.8, and 4.62, respectively. Mass-to-charge (m/z) transitions were as follows: 281.0 > 234.91 (D-luciferin), 306.03 > 259.98 (CycLuc1), 415.097 > 254.10 (Naltrindole). All compounds were extracted from biological samples by using protein precipitation method with ice cold acetonitrile. Since D-luciferin and CycLuc1 are light sensitive, all samples were stored in the dark and sample preparations performed under minimal exposure to the dim light. The lower limit of quantitation (LLOQ) for both D-luciferin and CycLuc1 was 2.5 ng/mL. The coefficients of variation for intra- and inter-assays accuracy and precision for both D-luciferin and CycLuc1 were less than 15%.

**Statistical analysis**

Data were presented as mean ± standard deviation (S.D.) or mean ± standard error of the estimate (S.E.) for the area under the curves. An unpaired two sample t-test was used to compare two groups in GraphPad Prism version 6.04 (GraphPad, La Jolla, CA) software with a significance level of $P < 0.05$.

DMD Fast Forward. Published on December 9, 2021 as DOI: 10.1124/dmd.121.000597
This article has not been copyedited and formatted. The final version may differ from this version.

## Results

### Comparison of BLI with D-luciferin and CycLuc1 in flank and intracranial tumors

Total flux of BLI light was compared using D-luciferin and CycLuc1 in the tumors implanted either on the flank (heterotopic model) or in the brain (orthotopic model) (Figure 2). GBM6, a GBM patient-derived xenograft (PDX), was stably transduced with a lentiviral construct carrying both td-tomato and a sequence optimized fLuc2 firefly luciferase gene. To enable a direct comparison between D-luciferin and CycLuc1, cross-over imaging was performed in the same mice on consecutive days for the flank and at two-day intervals for the brain. In the preliminary experiments, the order of imaging, i.e., either D-luciferin first or CycLuc1 first, was found not to affect the intensities of BLI signal for either compound, likely due to their short half-lives (less than 1 hour) (Figure S1). Therefore, cross-over imaging was performed on days 15, 21, and 28 for D-luciferin and on days 16, 22, and 29 for CycLuc1 after flank tumor implantation (*N*=5). In intracranial tumor models, BLI was performed on days 13, 19, and 26 for D-luciferin and on days 15, 21, and 28 for CycLuc1 after intracranial tumor injection (*N*=4). Two different doses of substrates were used for imaging: 30 and 150 mg/kg for D-luciferin and 5 and 25 mg/kg for CycLuc1. Overall intensities of the BLI signal were stronger in flank tumors when compared to intracranial tumors (Figure 2A and 2B). When the signal intensity from CycLuc1-mediated BLI was compared to that from D-luciferin-mediated BLI in the flank model, there was no significant difference between substrates when compared after low-dose administration or high-dose administration, respectively (Figure 2C and 2D). However, the signal intensity from CycLuc1-mediated BLI was significantly higher than that from D-luciferin-mediated in intracranial xenografts at either dose level (Figure 2E and 2F). The concentrations of these compounds were determined in different regions in the brain (Figure S2). The concentrations of both D-luciferin and CycLuc1 in the tumor core, defined by robust td-tomato signal, were more variable and higher compared to those in brain around tumor (BAT) or in normal brain (NB), even though

DMD Fast Forward. Published on December 9, 2021 as DOI: 10.1124/dmd.121.000597
This article has not been copyedited and formatted. The final version may differ from this version.

the average tissue to plasma ratios in all regions were below 2% for both D-luciferin and CycLuc1 (Figure S2). In the context of factors that can affect *in vivo* BLI signal intensity (Figure 1), these data, all based on light production, would initially suggest that distribution across the BBB into the brain may be a critical factor affecting the superiority of CycLuc1 imaging.

**Apparent permeability and efflux ratios of D-luciferin and CycLuc1**

Previous reports suggest that D-luciferin is an efflux substrate for Bcrp (Zhang et al., 2007; Bakhsheshian et al., 2013), and therefore the efflux liability for D-luciferin was compared to CycLuc1 in a standard bi-directional flux assay. The Papp of both D-luciferin and CycLuc1 were measured in both apical-to-basolateral (A-to-B) and basolateral-to-apical (B-to-A) directions using MDCKII vector control cells and MDCKII-Bcrp overexpressing cells cultured in a Transwell™ plate (Figure 3A). With vector control cells, there were no significant differences in the apparent permeabilities from apical to basolateral compartment when compared to those from basolateral to apical compartment with either D-luciferin or CycLuc1 (*N.S., P* > 0.05). However, the Papp from basolateral to apical compartments for both D-luciferin and CycLuc1 were significantly higher in Bcrp-overexpressing MDCKII cells than those from apical to basolateral compartments, indicative of a possible role of Bcrp on the biodistribution of these compounds ($P < 0.05$). The efflux ratios calculated for D-luciferin and CycLuc1 were 2.74 and 2.48, respectively, which demonstrated that both compounds were relatively weak (low affinity) substrates of the BBB efflux transporter, Bcrp. To further confirm this result, the effects of Bcrp inhibitor, Ko-143, was examined in MDCKII-Bcrp overexpressing cells. The Papp from B-to-A were measured in the presence of varying concentrations of Ko-143 from 0 to 100 μM. The results show that the B-to-A Papp proportionally decreased for both D-luciferin and CycLuc1 with increasing concentrations of the selective Bcrp inhibitor, Ko-143 (Figure 3B). The B-to-A Papp were significantly less in the presence of an inhibitor from that in the absence of an inhibitor ($*P < 0.05$).

DMD Fast Forward. Published on December 9, 2021 as DOI: 10.1124/dmd.121.000597
This article has not been copyedited and formatted. The final version may differ from this version.

**Comparison of pharmacokinetic parameters and metrics of D-luciferin and CycLuc1 in WT and BKO FVB mice following a single intravenous dose**

The plasma and brain concentration-time profiles of D-luciferin and CycLuc1 were obtained in both WT and BKO FVB mice following a single intravenous bolus administration (Figure 4A and 4B). Blood and brain were collected by serial sacrifice at 5 time points up to 60 minutes for D-luciferin, and 7 time points up to 180 minutes for CycLuc1, based on their previously-determined plasma half-lives. The concentrations of both D-luciferin and CycLuc1 in the BKO mice were higher at almost all time points when compared to the concentrations in WT for both plasma and brain. The pharmacokinetic parameters and metrics of both D-luciferin and CycLuc1 were calculated by non-compartmental analysis and are summarized in Table 1. The half-lives of D-luciferin in WT and BKO were 9.0 and 9.6 minutes, respectively. The half-lives of CycLuc1 in WT and BKO were 29.0 and 21.1 minutes, respectively; 2-3 times longer than D-luciferin in both genotypes, where the longer half-life of CycLuc1 may provide more consistent drug exposure among tested animals during the process of imaging through a more sustained systemic circulation at these tested doses. The volumes of distribution (Vd) of D-luciferin in both WT and BKO were much smaller (348 and 261 mL/kg in WT and BKO, respectively) than those of CycLuc1 (3430 and 2684 mL/kg in WT and BKO, respectively). The clearance (CL) of D-luciferin in WT (26.7 mL/min/kg) was higher than that in BKO (18.8 mL/min/kg), which possibly could be due to lack of efflux transporter in the elimination process of D-luciferin. Similarly, the CL of CycLuc1 in WT (82 mL/min/kg) was higher than that in BKO (61.3 mL/min/kg). As expected from the concentration-time profiles, the areas under the curve (AUCs) from time zero to the last time point of D-luciferin in the BKO plasma and BKO brain were significantly higher than those in WT (plasma: 1860 min*μg/mL in WT and 2608 min* μg/mL in BKO, $*P < 0.05$; brain: 9.19 min*μg/mL in WT and 19.2 min* μg/mL in BKO, $*P < 0.05$). CycLuc1 also showed results similar to D-luciferin, where the areas under the curve (AUCs) of both plasma and brain

DMD Fast Forward. Published on December 9, 2021 as DOI: 10.1124/dmd.121.000597
This article has not been copyedited and formatted. The final version may differ from this version.

in BKO were significantly higher than those in WT (plasma: 607 min*μg/mL in WT and 810 min*μg/mL in BKO, *$P$ < 0.05; brain: 1.87 min*μg/mL in WT and 2.80 min*μg/mL in BKO, *$P$ < 0.05). The partition coefficients of brain to plasma for both luciferase substrates were calculated by the ratios of AUCs from time zero to infinity in the brain to that in the plasma. For both D-luciferin and Cycluc1, the partition coefficients in BKO were slightly higher when compared to WT, but both values were extremely low; i.e., about 0.5% for D-luciferin and 0.3% for CycLuc1. The free brain partition coefficient values were determined from the free fraction obtained by using RED. The free brain partition coefficients of D-luciferin and CycLuc1 in both WT and BKO were also lower than unity. The calculated distribution advantages in BKO were less than 1.5 for both D-luciferin and CycLuc1, suggesting that the role of efflux transporter, Bcrp, in the brain distribution of these compounds is limited.

**Pharmacokinetics and tissue distribution of D-luciferin and CycLuc1 following a single intraperitoneal dose**

Because most laboratories use intraperitoneal administration of luciferin substrates, the concentrations in plasma and major tissues (brain, liver, kidney, heart, and intestine) over time were examined following a single intraperitoneal administration of either 150 mg/kg of D-luciferin or 20 mg/kg of CycLuc1 in WT FVB mice (Figure 5).

From the concentration-time profiles of plasma and brain, the elimination phase of D-luciferin has a mono-exponential decline, while the elimination phase of CycLuc1 has more of a bi-exponential decline. Similar to the results from intravenous administration, the half-lives of CycLuc1 in the plasma and the brain were about 3 times higher (Table 2, 31.4 minutes in the plasma and 38.8 minutes in the brain) than those of D-luciferin (10.9 minutes in plasma and 12.6 minutes in brain). The apparent volumes of distribution (Vd/F) were 240 and 334 mL/min/kg for D-luciferin and CycLuc1, respectively. The apparent clearances (CL/F) of D-luciferin and CycLuc1 seem to be similar, 15.3 and 18.9 mL/min/kg, respectively. The brain

DMD Fast Forward. Published on December 9, 2021 as DOI: 10.1124/dmd.121.000597
This article has not been copyedited and formatted. The final version may differ from this version.

partition coefficients ($Kp_{,brain}$) of D-luciferin and CycLuc1 were calculated by using the ratio of AUCs from time zero to infinity, and those were 0.5% for D-luciferin and 1.1% for CycLuc1. Similar to the results following an intravenous bolus dosing, the free brain partition coefficients were much lower than unity for both D-luciferin and CycLuc1.

Other tissue partition coefficients (Kps) were also calculated using the AUCs of each tissue from the concentration-time profiles. The partition coefficient was the highest in liver (10.3) for D-luciferin. On the contrary, for CycLuc1, the kidney has the highest tissue partition coefficient (7.5) (Table 3). The $Kp_{,brain}$ values for both D-luciferin and CycLuc1 were the lowest among all tissues analyzed and different from other tissue Kps. Therefore, the distribution of both D-luciferin and CycLuc1 was not restricted to the most peripheral tissues, except for the brain.

**Influence of co-administration of transporter inhibitors on the systemic clearance and the brain partition coefficients of D-luciferin and CycLuc1**

Efflux transporter inhibitors, Ko-143 (Bcrp selective) or probenecid (non-selective organic acid transporters inhibitor, e.g., OATs), was co-administered with D-luciferin or CycLuc1 in WT FVB mice to evaluate the role of selected efflux transporters on the brain distribution of D-luciferin and CycLuc1. Plasma and brain concentrations and brain-to-plasma ratios of D-luciferin and CycLuc1 following a co-administration with either Ko-143 or probenecid are presented in Figure 6. The concentrations of D-luciferin and CycLuc1 in both plasma and brain with the co-administration of Ko-143 were significantly increased at 60 minutes, but not at 10 minutes after dosing when compared to the D-luciferin/CycLuc1 only group (Figure 6A). Importantly, brain-to-plasma ratios did not differ with or without Ko-143 at each time point (Figure 6A, right). Similarly, the co-administration of probenecid with either D-luciferin or CycLuc1 significantly increased the concentrations of both compounds in the plasma at 60 minutes, but not at 10 minutes, after dosing (Figure 6B), while the brain concentrations were unaffected at each of these time-points. As a result, the brain-to- plasma ratios of D-luciferin and CycLuc1 were significantly decreased

DMD Fast Forward. Published on December 9, 2021 as DOI: 10.1124/dmd.121.000597
This article has not been copyedited and formatted. The final version may differ from this version.

with a co-administration of probenecid due to a significant increase in the plasma concentration at 60 minutes post-dose. In conclusion, co-administration of the Bcrp inhibitor and the inhibitor of OATs with either D-luciferin or CycLuc1 influenced the systemic clearance of these luciferase substrates.

## Discussion

BLI is a powerful noninvasive tool to determine the longitudinal growth of a tumor located in deep tissues or organs in preclinical cancer research (Lewis et al., 2002; Mook et al., 2003; Zeamari et al., 2004; Lyons, 2005). It is the most common method of measuring tumor size in orthotopic models, and often used as a guide to determine drug efficacy (Vassileva et al., 2008; Xi et al., 2012; Textor et al., 2014; Li et al., 2018). However, there have been concerns and difficulties of using BLI in brain tumor models, in part due to the limited brain delivery of luciferase substrate, D-luciferin (Genevois et al., 2016). A synthetic luciferase substrate, CycLuc1, has recently been described and has shown to produce a much stronger signal than D-luciferin from the brain at a dramatically lower dose (Evans et al., 2014). This novel BLI agent has been reported to have a greater potency than D-luciferin, based on its low $K_m$ for firefly luciferase (about 70-fold higher than D-luciferin); however, the quantitative brain distribution and pharmacokinetic properties of CycLuc1 have not been investigated (Harwood et al., 2011). The objective of the present study was to compare the bio-distribution of D-luciferin and CycLuc1 and understand the role of efflux transporters on the distribution and pharmacokinetics of these luciferase substrates, and resultant efficacy as BLI agents in the brain. This study shows that both D-luciferin and CycLuc1 are weak substrates of Bcrp. However, the role of Bcrp on the brain distribution of both substrates is limited based on our findings in both *in vitro* and *in*

DMD Fast Forward. Published on December 9, 2021 as DOI: 10.1124/dmd.121.000597
This article has not been copyedited and formatted. The final version may differ from this version.

*vivo* experiments using transporter transfected cell lines and transporter knockout mice. In particular, this conclusion was drawn based on the concentrations of both D-luciferin and CycLuc1 that were not inferred from the BLI signal intensity, but rather by direct quantitative measurement using a LC-MS/MS assay, in order to elucidate its delivery to the target area of imaging.

Comparison of BLI signal from using D-luciferin and CycLuc1 showed that the light signal from luciferase transfected brain tumors from CycLuc1 was significantly stronger (at practical and routine intraperitoneal doses) than the signal given by D-luciferin from tumors growing in the brain. This difference between these luciferase substrates was particularly important and highlighted by the fact that there was no significant difference in imaging signal intensities from the same tumors growing in the flank region, according to the cross-over imaging results. The stronger light signal in the brain with the use of CycLuc1 has been reported in luciferase-expressing mice by Evans et al. However, this study did not elucidate the reason for the stronger BLI signal from CycLuc1 (Evans et al., 2014). It is possible that CycLuc1, as speculated by Evans et al., may have better accessibility or distribution to the brain than D-luciferin. The similar BLI signal from the use of CycLuc1 or D-luciferin in flank tumors is consistent with the lack of distributional barrier in the peripheral region, such as flank tumor, as compared to tumors placed in the brain.

Apparent permeabilities of both D-luciferin and CycLuc1 *in vitro* were lower than $1 \times 10^{-6}$ cm/s, which is a common lower limit that indicates low intrinsic permeability (Artursson et al., 2001; Hubatsch et al., 2007), from A-to-B direction by using *in vitro* experiments with MDCKII wild-type and Bcrp overexpressing cell lines. Efflux ratios of D-luciferin and CycLuc1 using MDCKII Bcrp overexpressing cells indicate that Bcrp plays a role in the permeabilities of these luciferase substrates, even though the change in permeability was minor when compared to the underlying intrinsic permeability. Consistent with the conclusion from the efflux ratios, the

DMD Fast Forward. Published on December 9, 2021 as DOI: 10.1124/dmd.121.000597
This article has not been copyedited and formatted. The final version may differ from this version.

inhibition of Bcrp by Ko143 decreases apparent permeabilities of both D-luciferin and CycLuc1 from basolateral to apical compartment. However, even though the same concentration of Ko-143 decreases the permeability of D-luciferin more than that of CycLuc1 (1.7-fold decrease in D-luciferin, 1.1-fold decrease in CycLuc1 with 0.01 uM of Ko143 compared to the absence of an inhibitor), both reductions were not substantial, yet statistically significant (* $P < 0.05$). Interestingly, the transcellular permeabilities of both D-luciferin and CycLuc1 were found to be extremely low based on the results from *in vitro* cell uptake assays (results not shown), consistent with a previous report using D-luciferin (Lee et al., 2003). Therefore, the major distributional mechanism of D-luciferin and CycLuc1 to the organs and tissues is likely through a paracellular pathway of transport (similar to other hydrophilic compounds), and not a transcellular pathway affected by active transport. This is likely a primary reason why these compounds lack significant distribution into the brain and not peripheral organs and tissues (Figure 5 and Table 3), because the paracellular pathway of molecular transport is extremely limited at the blood-brain barrier, mainly due to the high expression of tight and adherens junctions confirmed by a high electrical resistance (Butt et al., 1990). Bcrp, expressed on the luminal side of brain endothelial cells, transports compounds from inside the brain capillary endothelial cells or from within the lipid bilayer of luminal cell membrane (Kubo et al., 2015). These findings may explain why Bcrp has a limited role in the distribution of both D-luciferin and CycLuc1 to the brain. Moreover, since polar compounds like D-luciferin and CycLuc1 have a low intrinsic permeability, the substrate concentration accessible to the transporter will be limited, and in conjunction with a low transporter affinity for each compound, the Bcrp-mediated transport rate could be low irrespective of the transport capacity across the BBB.

*In vivo* experiments using WT and BKO FVB mice showed the limited role of Bcrp at the BBB on the brain distribution of D-luciferin and CycLuc1. The brain partition coefficients of D-luciferin and CycLuc1 in BKO did not show significant changes from those in WT. However, the

DMD Fast Forward. Published on December 9, 2021 as DOI: 10.1124/dmd.121.000597
This article has not been copyedited and formatted. The final version may differ from this version.

AUCs of both plasma and brain concentrations for D-luciferin and CycLuc1 were significantly higher in BKO when compared to WT. The genetic deletion of Bcrp changed the overall systemic exposure to D-luciferin and CycLuc1 by decreasing the systemic clearances (Table 1). It has been reported that D-luciferin is eliminated mainly by kidney and hepato-biliary system, based on the biodistribution of radiolabeled D-luciferin (Lee et al., 2003; Berger et al., 2008). Therefore, the results from BKO and WT indicate that Bcrp plays a significant role in how the kidney and liver eliminate luciferin, likely through active secretory processes at the kidney tubule and bile canaliculus, but not in the distribution to the brain. There can be several possible reasons to explain why the lack of Bcrp does not change the brain partition coefficient in mice. First, there may be other efflux transporters besides Bcrp, possibly multidrug resistance-associated proteins (MRPs) or OATs known to transport organic anions. It has been reported that D-luciferin is a substrate of MRP4 (Cheung et al., 2015). Considering that both D-luciferin and CycLyc1 have a carboxylic acid group, which has an anionic charge at physiological pH, these OATs may be involved in the brain distribution of these luciferase substrates at the BBB. Either MRPs and/or OATs, given the results of the probenecid inhibition studies (Figure 6B), are involved in the elimination of both D-luciferin and CycLuc1, even though inhibition of OAT by probenecid does not lead to an increase in brain partition coefficients. Second, upon examining the results of the ko-143 inhibition studies, the role of Bcrp may be limited in this case, especially at the BBB, due to low intrinsic permeability of the substrates to cross the BBB, as outlined above by the *in vitro* permeability experiments. Intrinsic permeability, driven by diffusion, may consist of a transcellular pathway and a paracellular pathway of molecular transport. As previously mentioned, the transcellular diffusive pathway minimally contributes to the overall molecular transport for the polar substrates, D-luciferin and CycLuc1. Due to of the restricted paracellular transport at the BBB due to the presence of intact tight junctions, transport of polar molecules, such as D-luciferin and CycLuc1, into the brain is expected to be limited. Therefore, overall permeabilities of D-luciferin and CycLuc1 across the BBB are

DMD Fast Forward. Published on December 9, 2021 as DOI: 10.1124/dmd.121.000597
This article has not been copyedited and formatted. The final version may differ from this version.

extremely low regardless of the activity of Bcrp. This is consistent with the general understanding that substrates of active efflux transporters are mostly lipophilic compounds (Golden and Pollack, 2003). Hydrophilic compounds like D-luciferin and CycLuc1 are reported to be less influenced by active efflux transporters (Abbott, 2013). On the other hand, the activity of Bcrp becomes more pronounced in the eliminating organs (kidney and liver), because permeabilities are great enough to allow the substrates ready access to the transporter, and as such the efflux activity of Bcrp is important. Moreover, the activity of Bcrp is reported to be dependent on the pH by changing the effective ionization state of its substrates (Li et al., 2011). The ionization of carboxylic acid on D-luciferin and CycLuc1 at physiological pH influences the activity of Bcrp on these substrates. Similar phenomena have been observed with methotrexate, pemetrexed, and fluorescein, which are all hydrophilic compounds with low permeabilities (Sun et al., 2001; Li et al., 2013; Sane et al., 2014). Methotrexate is a hydrophilic compound with low XLogP of -1.8 and a substrate of Bcrp (Sane et al., 2014), and its apparent permeability is reported to be 1.2 X $10^{-6}$ cm/sec in Caco-2 cells, that is similar to D-luciferin and CycLuc1 (Yee, 1997). According to Sane et al., the absence of Bcrp in *Abcg2*$^{-/-}$ mice increases both the plasma and brain exposure of methotrexate, which results in a minor (statistically not significant) increase in brain to plasma ratios. Interestingly, methotrexate is a substrate of both Bcrp and MRP4, so there was a statistically significant increase in $Kp_{,brain}$ with double knockout mice that lack both Bcrp and MRP4, but the result was only 2-fold higher. Therefore, it is also possible that other efflux transporters are involved in the brain distribution of D-luciferin and CycLuc1, as in the example of methotrexate.

D-luciferin has been previously reported to be a substrate of Bcrp (Zhang et al., 2007; Bakhsheshian et al., 2013). Bakhsheshian et al., have shown that co-administration of the Bcrp inhibitor, Ko-143, increased the BLI output from the brain in mice without significant changes in the concentration of D-luciferin in plasma at 10-minutes after dosing (Bakhsheshian et al.,

DMD Fast Forward. Published on December 9, 2021 as DOI: 10.1124/dmd.121.000597
This article has not been copyedited and formatted. The final version may differ from this version.

2013). The results from the current study are not fully consistent with the conclusions of Bakhsheshain et al., since the co-administration of Ko-143 was not able to significantly increase the concentration of D-luciferin in the brain at 10-minute after the dosing with the same dose and dosing schedule as used by Bakhsheshian et al. However, there was a significant increase in both plasma and brain concentrations of D-luciferin at 60 minutes after the dosing, even though the brain-to-plasma ratios of the inhibitor treated group were not significantly different from the ones of the luciferase substrate only group (Figure 6). These results prompted us to ask what would be the reasons that may lead to a discrepancy between these two experiments. The only difference between these experiments is the method of "estimating" the D-luciferin concentrations in the brain and plasma specimens. The concentrations of both D-luciferin and CycLuc1 were determined by LC-MS/MS in the present study. In Bakhsheshian et al., the concentrations of D-luciferin in the brain and plasma were assumed to be directly proportional to the measured BLI light intensity (Bakhsheshian et al., 2013). As discussed earlier, the intensity of light signal can be affected by several factors other than the concentration of substrate itself (Figure 1). Moreover, the intensity of BLI light signal that is the product of enzyme reaction does not always have a direct linear correlation with the concentration of substrates. According to the Michaelis-Menten kinetics on the enzyme reaction, small changes in the substrate concentration can be resulted in large changes in the response depending on the affinity of enzyme to a substrate. Therefore, a direct correlation may not adequately describe the relationship between the light signal intensity and the concentration of D-luciferin. Even though both D-luciferin and CycLuc1 are undoubtedly substrates of Bcrp, the question arises whether the use of Bcrp inhibitors can substantially modulate the brain distribution of these luciferase substrates. Consistent with the results from BKO mice, the role of the efflux transporter, Bcrp, at the BBB is limited, due to its low intrinsic permeability across the BBB from the beginning. Therefore, the inhibition of Bcrp increased the systemic exposure, and as such, increased the driving force for

DMD Fast Forward. Published on December 9, 2021 as DOI: 10.1124/dmd.121.000597
This article has not been copyedited and formatted. The final version may differ from this version.

distribution to the brain of these compounds, a result not necessarily due to the role of efflux transporters, such as Bcrp, at the BBB.

Unlike D-luciferin, there is limited data available regarding the biodistribution and substrate status of CycLuc1 to understand the mechanism of enhanced light emission (Evans et al., 2014). There was speculation that the brain distribution and intrinsic permeability of CycLuc1 would be better than D-luciferin, based on the higher XLogP value of CycLuc1 when compared to D-luciferin. However, the current study has clarified that the biodistribution, especially the brain distribution, of both D-luciferin and CycLuc1 are similar. Moreover, both compounds are weak substrates of Bcrp. The reason that CycLuc1 does not have any advantage on the permeability and brain distribution over D-luciferin is likely due to a free carboxylate of both compounds which is ionized at physiological pH, thus resulting in the similar cLogD. The presence of ionized carboxylate is required to be a substrate of fLuc, but it is a major limiting factor for cell permeability and brain penetration. There has been an interesting study of making a pro-drug of luciferin to avoid the problem with carboxylic acid (Mofford and Miller, 2015). Mofford et al. have reported that luciferin amides improve brain BLI in live mice over their parent luciferins. The current study, combined with the previous findings, provide possible explanations on why CycLuc1 has a more robust BLI signal and how it can be further improved.

In summary, the present study examined the pharmacokinetics, brain distribution, and the role of active efflux transporters on luciferase substrates, D-luciferin and CycLuc1. The results showed the distributional factors influencing the BLI signal that are related to the brain distribution of the substrates. Even though D-luciferin and CycLuc1 have similar physicochemical properties, CycLuc1 would be a better substrate of firefly luciferase for imaging intracranial tumors, mainly due to its superior affinity to firefly luciferase, and intrinsic enhanced relative quantum yield (Reddy et al., 2010). The current paper suggests that the role of Bcrp is limited on the brain distribution of both D-luciferin and CycLuc1, in part because these luciferase

DMD Fast Forward. Published on December 9, 2021 as DOI: 10.1124/dmd.121.000597
This article has not been copyedited and formatted. The final version may differ from this version.

substrates are only weak substrates of Bcrp and that superior imaging outcome from the use of CycLuc1 are driven by other intrinsic and pharmacokinetic properties.



**ACKNOWLEDGEMENTS**

The authors thank Jim Fisher, Clinical Pharmacology Analytical Laboratory, University of Minnesota, for his support in the development of the LC-MS/MS assays.

**AUTHORSHIP CONTRIBUTIONS**

Participated in research design: Kim, Gupta, Sarkaria, Elmquist

Conducted experiments: Kim, Gupta, Talele, Mohammad, Laramy, Mladek, S. Zhang

Performed data analysis: Kim, Gupta, W. Zhang, Sarkaria, Elmquist

Wrote or contributed to the writing of the manuscript: Kim, Laramy, Gupta, W. Zhang, Sarkaria, Elmquist

## References

Abbott NJ (2013) Blood-brain barrier structure and function and the challenges for CNS drug delivery. *J Inherit Metab Dis* **36:**437-449.

Artursson P, Palm K, and Luthman K (2001) Caco-2 monolayers in experimental and theoretical predictions of drug transport. *Adv Drug Deliv Rev* **46:**27-43.

Bakhsheshian J, Wei BR, Chang KE, Shukla S, Ambudkar SV, Simpson RM, Gottesman MM, and Hall MD (2013) Bioluminescent imaging of drug efflux at the blood-brain barrier mediated by the transporter ABCG2. *Proc Natl Acad Sci U S A* **110:**20801-20806.

Berger F, Paulmurugan R, Bhaumik S, and Gambhir SS (2008) Uptake kinetics and biodistribution of 14C-D-luciferin--a radiolabeled substrate for the firefly luciferase catalyzed bioluminescence reaction: impact on bioluminescence based reporter gene imaging. *Eur J Nucl Med Mol Imaging* **35:**2275-2285.

Butt AM, Jones HC, and Abbott NJ (1990) Electrical resistance across the blood-brain barrier in anaesthetized rats: a developmental study. *J Physiol* **429:**47-62.

Cheung L, Yu DM, Neiron Z, Failes TW, Arndt GM, and Fletcher JI (2015) Identification of new MRP4 inhibitors from a library of FDA approved drugs using a high-throughput bioluminescence screen. *Biochem Pharmacol* **93:**380-388.

Dawson JB, Barker DJ, Ellis DJ, Grassam E, Cotterill JA, Fisher GW, and Feather JW (1980) A theoretical and experimental study of light absorption and scattering by in vivo skin. *Phys Med Biol* **25:**695-709.

Evans MS, Chaurette JP, Adams ST, Jr., Reddy GR, Paley MA, Aronin N, Prescher JA, and Miller SC (2014) A synthetic luciferin improves bioluminescence imaging in live mice. *Nat Methods* **11:**393-395.

Genevois C, Loiseau H, and Couillaud F (2016) In Vivo Follow-up of Brain Tumor Growth via Bioluminescence Imaging and Fluorescence Tomography. *Int J Mol Sci* **17**.

Golden PL and Pollack GM (2003) Blood-brain barrier efflux transport. *J Pharm Sci* **92:**1739-1753.

Harwood KR, Mofford DM, Reddy GR, and Miller SC (2011) Identification of mutant firefly luciferases that efficiently utilize aminoluciferins. *Chem Biol* **18:**1649-1657.

Hubatsch I, Ragnarsson EG, and Artursson P (2007) Determination of drug permeability and prediction of drug absorption in Caco-2 monolayers. *Nat Protoc* **2:**2111-2119.

Jathoul AP, Grounds H, Anderson JC, and Pule MA (2014) A dual-color far-red to near-infrared firefly luciferin analogue designed for multiparametric bioluminescence imaging. *Angew Chem Int Ed Engl* **53:**13059-13063.

Kalvass JC and Maurer TS (2002) Influence of nonspecific brain and plasma binding on CNS exposure: implications for rational drug discovery. *Biopharm Drug Dispos* **23:**327-338.

Kaskova ZM, Tsarkova AS, and Yampolsky IV (2016) 1001 lights: luciferins, luciferases, their mechanisms of action and applications in chemical analysis, biology and medicine. *Chem Soc Rev* **45:**6048-6077.

Kim M, Ma DJ, Calligaris D, Zhang S, Feathers RW, Vaubel RA, Meaux I, Mladek AC, Parrish KE, Jin F, Barriere C, Debussche L, Watters J, Tian S, Decker PA, Eckel-Passow JE, Kitange GJ, Johnson AJ, Parney IF, Anastasiadis PZ, Agar NYR, Elmquist WF, and Sarkaria JN (2018) Efficacy of the MDM2 Inhibitor SAR405838 in Glioblastoma Is Limited by Poor Distribution Across the Blood-Brain Barrier. *Mol Cancer Ther* **17:**1893-1901.

Kubo Y, Ohtsuki S, Uchida Y, and Terasaki T (2015) Quantitative Determination of Luminal and Abluminal Membrane Distributions of Transporters in Porcine Brain Capillaries by Plasma Membrane Fractionation and Quantitative Targeted Proteomics. *J Pharm Sci* **104:**3060-3068.

Laramy JK, Kim M, Gupta SK, Parrish KE, Zhang S, Bakken KK, Carlson BL, Mladek AC, Ma DJ, Sarkaria JN, and Elmquist WF (2017) Heterogeneous Binding and Central Nervous System Distribution of the

Multitargeted Kinase Inhibitor Ponatinib Restrict Orthotopic Efficacy in a Patient-Derived Xenograft Model of Glioblastoma. *J Pharmacol Exp Ther* **363:**136-147.

Lee KH, Byun SS, Paik JY, Lee SY, Song SH, Choe YS, and Kim BT (2003) Cell uptake and tissue distribution of radioiodine labelled D-luciferin: implications for luciferase based gene imaging. *Nucl Med Commun* **24:**1003-1009.

Lewis JS, Achilefu S, Garbow JR, Laforest R, and Welch MJ (2002) Small animal imaging. current technology and perspectives for oncological imaging. *Eur J Cancer* **38:**2173-2188.

Li L, Agarwal S, and Elmquist WF (2013) Brain efflux index to investigate the influence of active efflux on brain distribution of pemetrexed and methotrexate. *Drug Metab Dispos* **41:**659-667.

Li L, Sham YY, Bikadi Z, and Elmquist WF (2011) pH-Dependent transport of pemetrexed by breast cancer resistance protein. *Drug Metab Dispos* **39:**1478-1485.

Li Y, Du Y, Sun T, Xue H, Jin Z, and Tian J (2018) PD-1 blockade in combination with zoledronic acid to enhance the antitumor efficacy in the breast cancer mouse model. *BMC Cancer* **18:**669.

Lyons SK (2005) Advances in imaging mouse tumour models in vivo. *J Pathol* **205:**194-205.

Mofford DM and Miller SC (2015) Luciferins behave like drugs. *ACS Chem Neurosci* **6:**1273-1275.

Mook OR, Van Marle J, Vreeling-Sindelarova H, Jonges R, Frederiks WM, and Van Noorden CJ (2003) Visualization of early events in tumor formation of eGFP-transfected rat colon cancer cells in liver. *Hepatology* **38:**295-304.

Reddy GR, Thompson WC, and Miller SC (2010) Robust Light Emission from Cyclic Alkylaminoluciferin Substrates for Firefly Luciferase. *Journal of the American Chemical Society* **132:**13586-13587.

Sane R, Wu SP, Zhang R, and Gallo JM (2014) The effect of ABCG2 and ABCC4 on the pharmacokinetics of methotrexate in the brain. *Drug Metab Dispos* **42:**537-540.

Sun H, Miller DW, and Elmquist WF (2001) Effect of probenecid on fluorescein transport in the central nervous system using in vitro and in vivo models. *Pharm Res* **18:**1542-1549.

Textor A, Listopad JJ, Wuhrmann LL, Perez C, Kruschinski A, Chmielewski M, Abken H, Blankenstein T, and Charo J (2014) Efficacy of CAR T-cell therapy in large tumors relies upon stromal targeting by IFNgamma. *Cancer Res* **74:**6796-6805.

Thorne N, Inglese J, and Auld DS (2010) Illuminating insights into firefly luciferase and other bioluminescent reporters used in chemical biology. *Chem Biol* **17:**646-657.

Vassileva V, Moriyama EH, De Souza R, Grant J, Allen CJ, Wilson BC, and Piquette-Miller M (2008) Efficacy assessment of sustained intraperitoneal paclitaxel therapy in a murine model of ovarian cancer using bioluminescent imaging. *Br J Cancer* **99:**2037-2043.

Weissleder R and Ntziachristos V (2003) Shedding light onto live molecular targets. *Nat Med* **9:**123-128.

Xi G, Rajaram V, Mania-Farnell B, Mayanil CS, Soares MB, Tomita T, and Goldman S (2012) Efficacy of vincristine administered via convection-enhanced delivery in a rodent brainstem tumor model documented by bioluminescence imaging. *Childs Nerv Syst* **28:**565-574.

Yee S (1997) In vitro permeability across Caco-2 cells (colonic) can predict in vivo (small intestinal) absorption in man--fact or myth. *Pharm Res* **14:**763-766.

Zeamari S, Rumping G, Floot B, Lyons S, and Stewart FA (2004) In vivo bioluminescence imaging of locally disseminated colon carcinoma in rats. *Br J Cancer* **90:**1259-1264.

Zhang Y, Bressler JP, Neal J, Lal B, Bhang HE, Laterra J, and Pomper MG (2007) ABCG2/BCRP expression modulates D-Luciferin based bioluminescence imaging. *Cancer Res* **67:**9389-9397.

DMD Fast Forward. Published on December 9, 2021 as DOI: 10.1124/dmd.121.000597
This article has not been copyedited and formatted. The final version may differ from this version.

## COMPETING INTERESTS

The authors declare no competing interests.

## DATA AVAILABILITY

All data generated or analyzed during this study are included in this published article (and its Supplementary Information files).

## FOOTNOTES

This work was supported by the National Institutes of Health [Grants RO1 CA138437, RO1 NS077921, U54 CA210181, U01 CA227954 and P50 CA108960].

## Figure Legends

Figure1. Schematic depiction of factors influencing BLI light signal.

Figure 2. BLI of GBM6 in flank tumor (A, C, D) and intracranial tumor (B, E, F) models. Cross-over imaging was performed for both substrate D-luciferin and CycLuc1 on different days.

Figure 3. *In vitro* apparent permeability measurement of D-luciferin and CycLuc1 in MDCKII-Bcrp overexpressing (BCRP) cell lines (A) or in the presence of Bcrp inhibitor Ko-143 (B). *(* P-value < 0.05 in (B) compared with control group)*

Figure 4. Concentration-time profiles of D-luciferin (A) and CycLuc1 (B) in plasma and brain following a single intravenous dose (D-luciferin, 50 mg/kg; CycLuc1, 20 mg/kg) in WT and BKO FVB mice.

DMD Fast Forward. Published on December 9, 2021 as DOI: 10.1124/dmd.121.000597
This article has not been copyedited and formatted. The final version may differ from this version.

Figure 5. Concentration-time profiles of D-luciferin (A) and CycLuc1 (B) in plasma and major tissues following a single intraperitoneal injection (D-luciferin, 150 mg/kg; CycLuc1, 20 mg/kg) in WT FVB mice.

Figure 6. Plasma and brain concentrations and brain-to-plasma ratios of D-luciferin (50 mg/kg) and CycLuc1 (10 mg/kg) at two time points in WT mice with a co-administration of either 16 mg/kg of Ko-143 (A) or 150 mg/kg of probenecid (B).

DMD Fast Forward. Published on December 9, 2021 as DOI: 10.1124/dmd.121.000597
This article has not been copyedited and formatted. The final version may differ from this version.

## Tables

### Table 1

Summary of pharmacokinetic parameters and metrics following a single intravenous dose of either D-luciferin or CycLuc1 in WT and BKO FVB mice

| | D-luciferin | | | | CycLuc1 | | | |
|---|---|---|---|---|---|---|---|---|
| | Plasma | | Brain | | Plasma | | Brain | |
| | WT | BKO | WT | BKO | WT | BKO | WT | BKO |
| t1/2 (min) | 9.01 | 9.59 | 11.8 | 7.69 | 29.0 | 21.1 | 38.3 | 23.8 |
| Dose (mg/kg) | 50 | 50 | - | - | 20 | 20 | - | - |
| $AUC_{0-t}$ (min*ug/mL) | 1860±117 | 2608±139 (*) | 9.03±0.819 | 9.1±1.97 (*) | 607±25.2 | 810±106 (*) | 1.84±0.199 | 2.80±0.298 (*) |
| $AUC_{0-\infty}$ (min*ug/mL) | 1869 | 2653 | 9.19 | 9.20 | 610 | 815 | 1.87 | 2.97 |
| Vd (mL/kg) | 348 | 261 | - | - | 3430 | 2684 | - | - |
| CL (mL/min/kg) | 26.7 | 18.8 | - | - | 82.0 | 61.3 | - | - |
| $Kp_{,brain}$ | - | - | 0.0049 | 0.0035 | - | - | 0.0031 | 0.0036 |
| fu | 0.512 | | 0.307 | | 0.360 | | 0.152 | |
| $Kp_{uu,brain}$ | - | - | 0.0029 | 0.0021 | - | - | 0.0013 | 0.0015 |
| Distribution Advantage (DA) | - | - | 1 | 0.72 | - | - | 1 | 1.2 |

* *P<0.05*

$t_{1/2}$, half life; $AUC_{0-t}$, area under the curve from zero to the time of last measured concentration; $AUC_{0-\infty}$, area under the curve from zero to time infinity; Vd, volume of distribution; CL, clearance; $Kp_{,brain}$ (AUC ratio), the ratio of $AUC_{(0-\infty,brain)}$ to $AUC_{(0-\infty,plasma)}$ using total drug concentrations; fu, free fraction; $Kp_{uu,brain}$ (AUC ratio), the ratio of $AUC_{(0-\infty,brain)}$ to $AUC_{(0-\infty,plasma)}$ using free drug concentrations; DA (Distribution advantage), the ratio of $Kp_{knockout}$ to $Kp_{WT}$.

DMD Fast Forward. Published on December 9, 2021 as DOI: 10.1124/dmd.121.000597
This article has not been copyedited and formatted. The final version may differ from this version.

## Table 2

Summary of pharmacokinetic parameters and metrics following a single intraperitoneal dose of either D-luciferin or CycLuc1 in WT FVB mice.

| | D-luciferin | | CycLuc1 | |
|---|---|---|---|---|
| | Plasma | Brain | Plasma | Brain |
| $t_{1/2}$ (min) | 10.9 | 12.6 | 31.4 | 38.8 |
| Dose (mg/kg) | 150 | - | 20 | - |
| $AUC_{0-t}$ (min*ug/mL) | 9784±1362 | 47.5±7.17 | 339±68.3 | 2.72±0.221 |
| $AUC_{0-\infty}$ (min*ug/mL) | 9830 | 48.13 | 364 | 3.97 |
| F (%) | 176 | | 60 | |
| Vd/F (mL/kg) | 240 | - | 334 | - |
| CL/F (mL/min/kg) | 15.3 | - | 18.9 | - |
| $Kp_{,brain}$ | - | 0.0049 | - | 0.0109 |
| fu | 0.512 | 0.307 | 0.360 | 0.152 |
| $Kp_{uu,brain}$ | - | 0.0029 | - | 0.0046 |

$t_{1/2}$, half life; $AUC_{0-t}$, area under the curve from zero to the time of last measured concentration; $AUC_{0-\infty}$, area under the curve from zero to time infinity; F, bioavailability; Vd/F, apparent volume of distribution; CL/F, apparent clearance; $Kp_{,brain}$ (AUC ratio), the ratio of $AUC_{(0-\infty,brain)}$ to $AUC_{(0-\infty,plasma)}$ using total drug concentrations; fu, free fraction; $Kp_{uu,brain}$ (AUC ratio), the ratio of $AUC_{(0-\infty,brain)}$ to $AUC_{(0-\infty,plasma)}$ using free drug concentrations.

## Table 3

The areas under the curve (AUCs) and calculated partition coefficients (Kp) of tissues following a single intraperitoneal dose of D-luciferin and CycLuc1

| | | Plasma | Brain | Heart | Liver | Kidney | Intestine |
|---|---|---|---|---|---|---|---|
| D-luciferin | $AUC_{0-\infty}$ (min*ug/mL) | 9830 | 48 | 47332 | 101666 | 9687 | 11335 |
| | Kp | - | 0.0049 | 4.82 | 10.3 | 0.985 | 1.15 |
| CycLuc1 | $AUC_{0-\infty}$ (min*ug/mL) | 364 | 3.97 | 9.38 | 458 | 2722 | 271 |
| | Kp | - | 0.0109 | 0.0258 | 1.26 | 7.48 | 0.745 |

$AUC_{0-\infty}$, area under the curve from zero to time infinity; Kp (AUC ratio), the ratio of $AUC_{(0-\infty,tissue)}$ to $AUC_{(0-\infty,plasma)}$ using total drug concentrations.

DMD Fast Forward. Published on December 9, 2021 as DOI: 10.1124/dmd.121.000597
This article has not been copyedited and formatted. The final version may differ from this version.

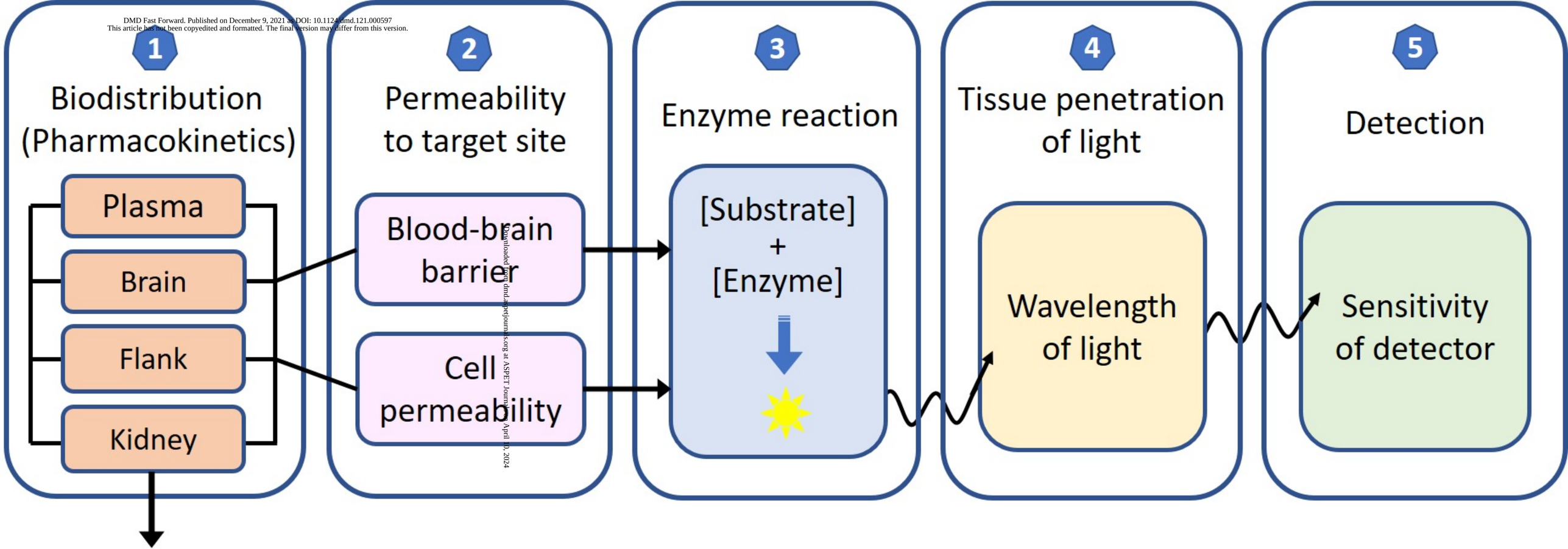




Figure 1

# Figure 2

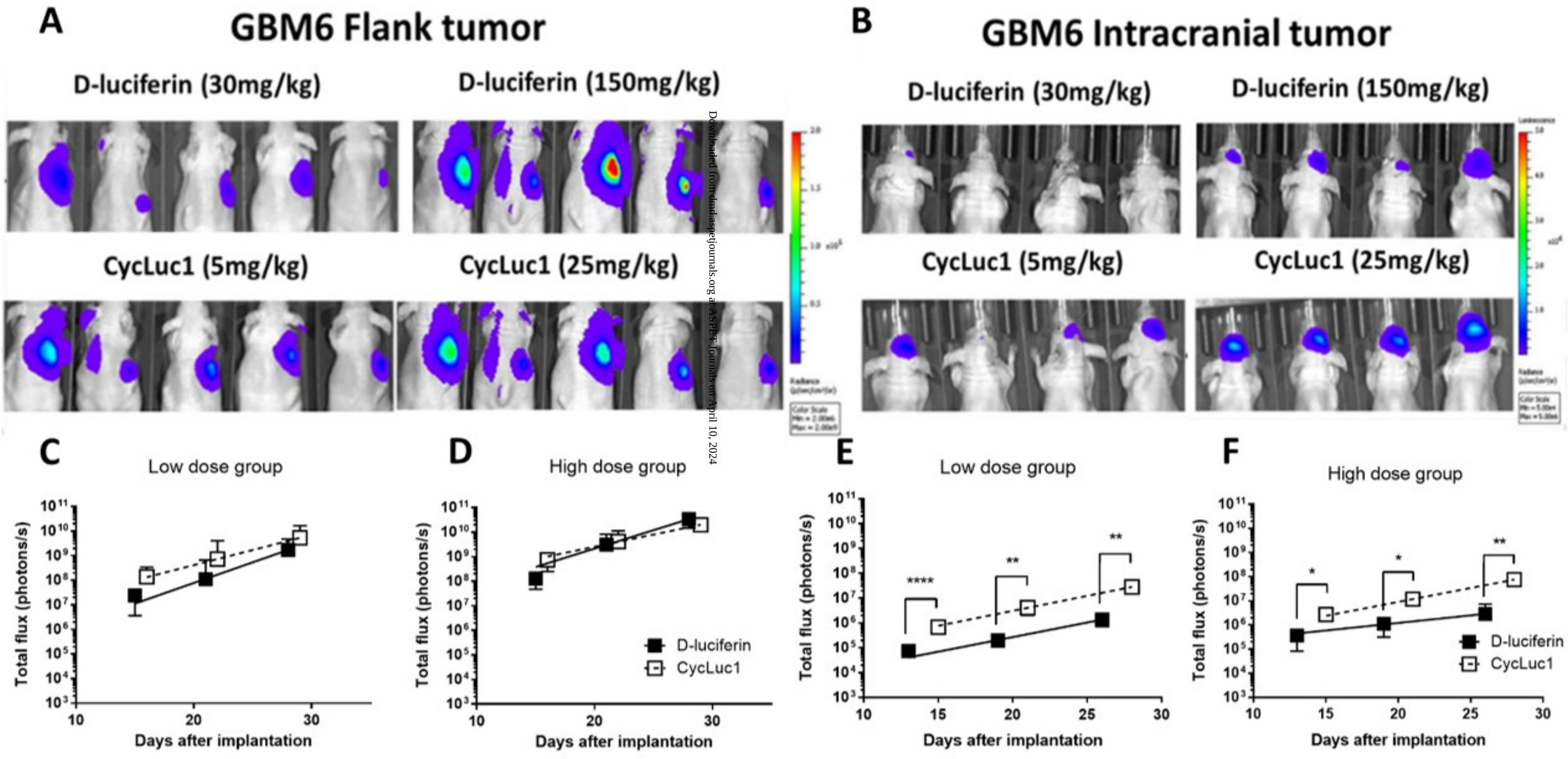

# Figure 3



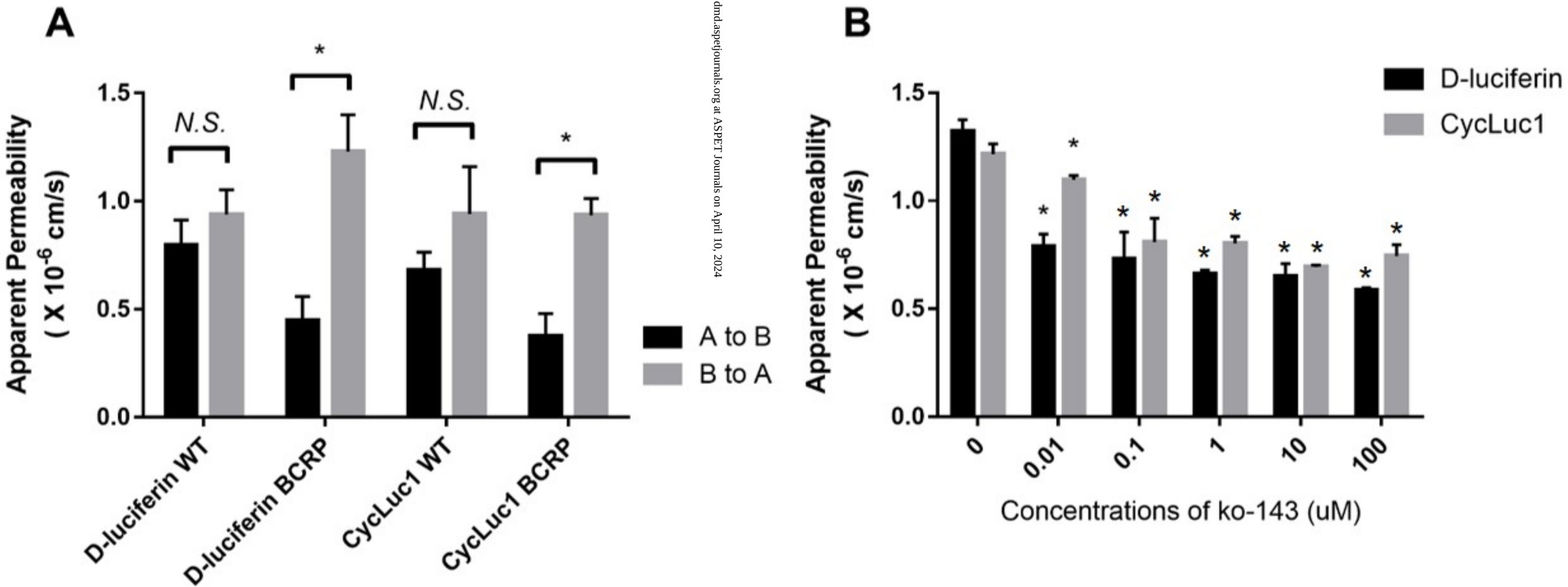

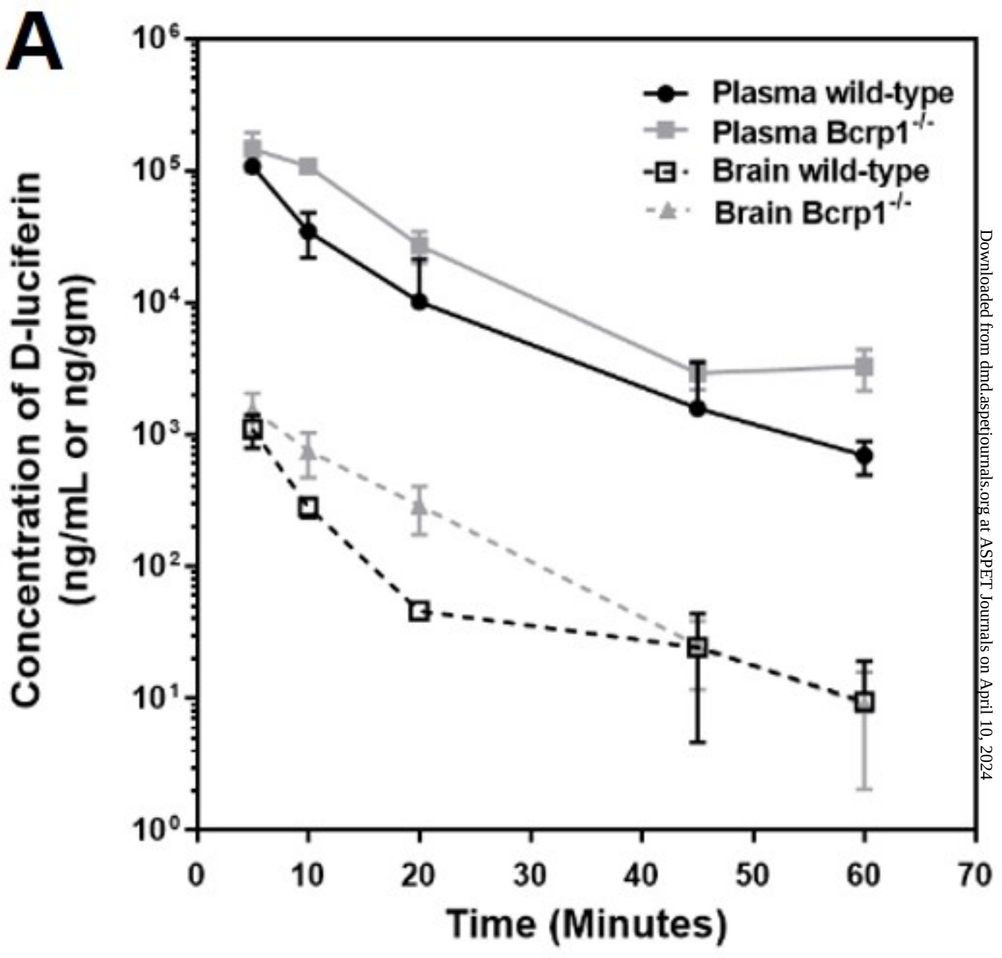




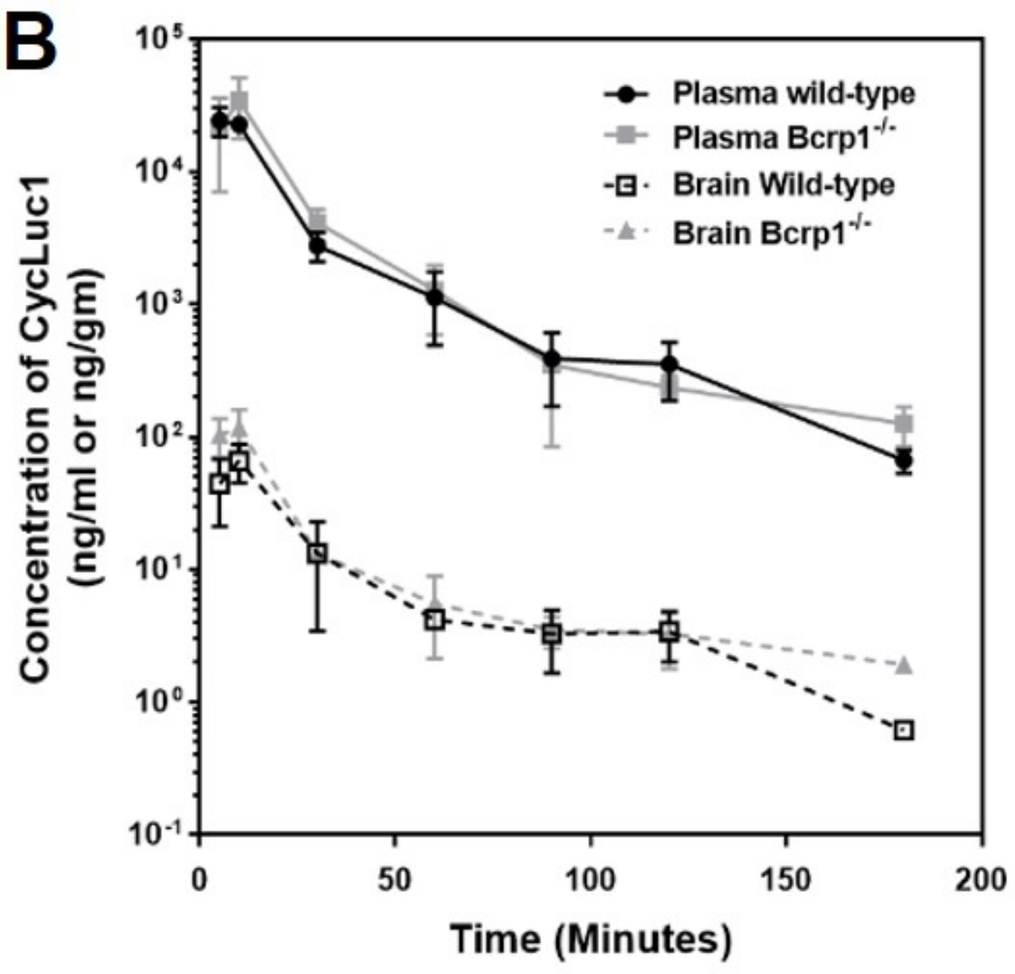


Figure 4

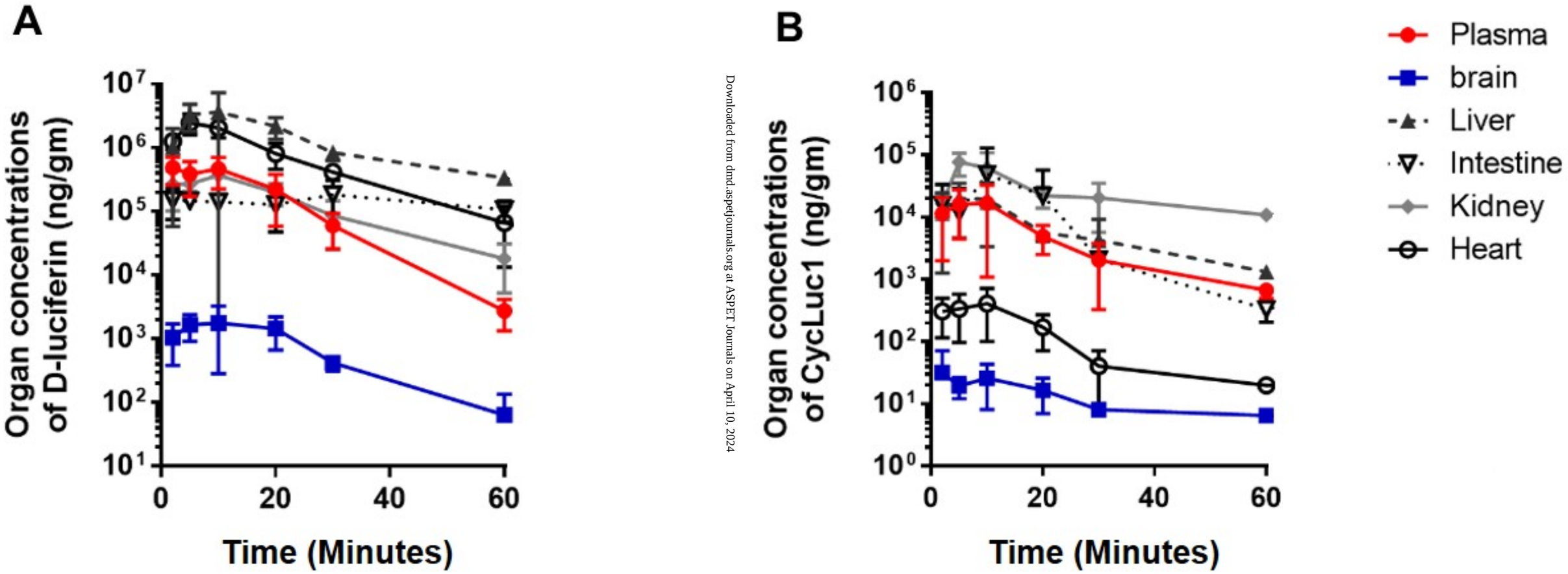




Figure 5

DMD Fast Forward. Published on December 9, 2021 as DOI: 10.1124/dmd.121.000597
This article has not been copyedited and formatted. The final version may differ from this version.

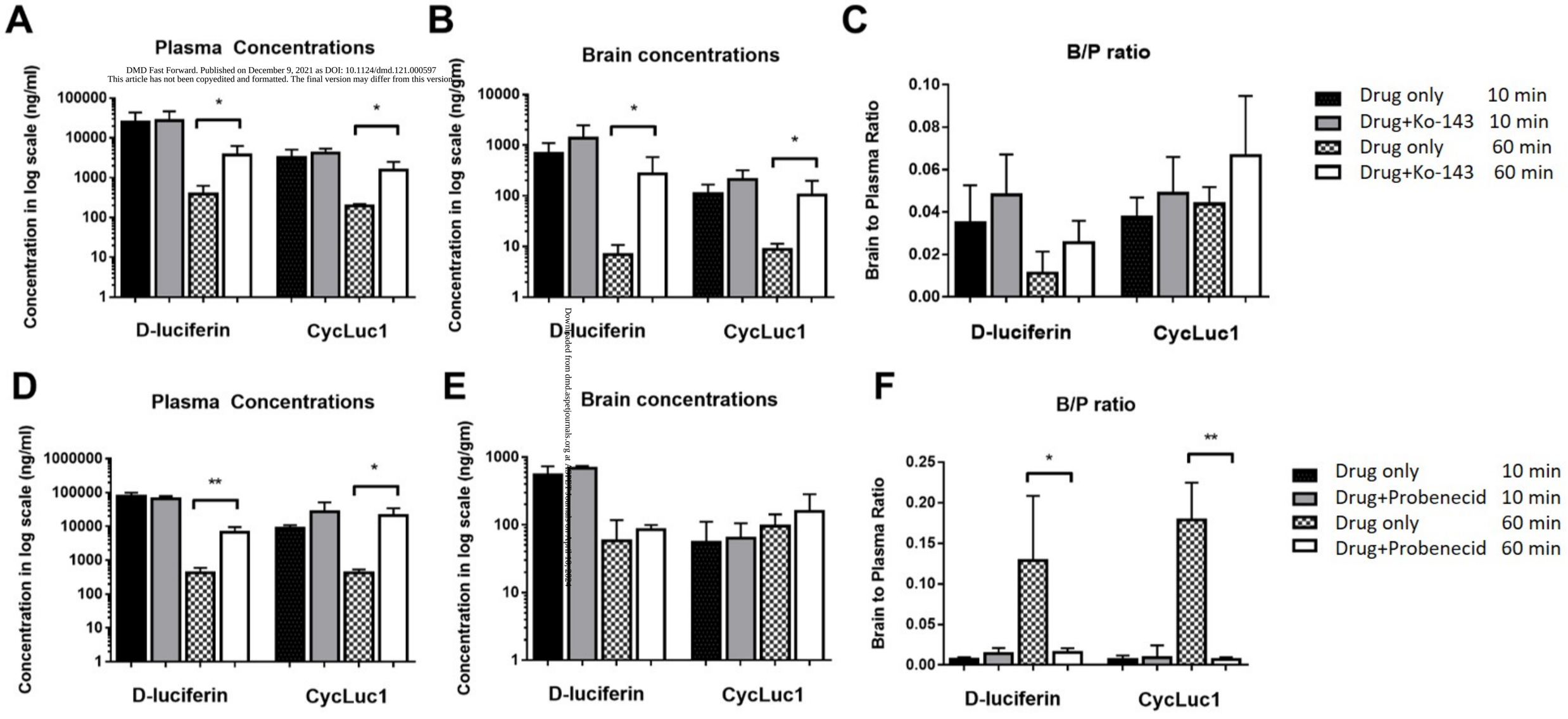




Figure 6